Validation of the computational model of a coronary stent: A fundamental step towards in silico trials

Luca Antonini, Lorenzo Mandelli, Francesca Berti, Giancarlo Pennati, Lorenza Petrini

PII: S1751-6161(21)00322-2

DOI: https://doi.org/10.1016/j.jmbbm.2021.104644

Reference: JMBBM 104644

To appear in: *Journal of the Mechanical Behavior of Biomedical Materials*

Received Date: 2 August 2020

Revised Date: 22 April 2021

Accepted Date: 9 June 2021

Please cite this article as: Antonini, L., Mandelli, L., Berti, F., Pennati, G., Petrini, L., Validation of the computational model of a coronary stent: A fundamental step towards in silico trials, *Journal of the Mechanical Behavior of Biomedical Materials* (2021), doi: https://doi.org/10.1016/j.jmbbm.2021.104644.

In silico trial: deployment steps and outputs

Are the results reliable?

A preliminary validation process of the delivery system numerical model is required

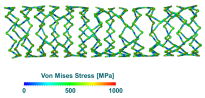

Delivery system:
two numerical strategies (Str_VP, Str_MS)

2) Uniaxial tensile post-expansion tests

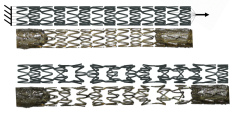

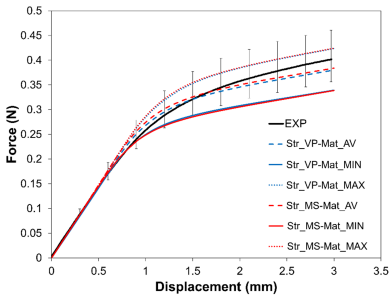

1) Free-expansion tests

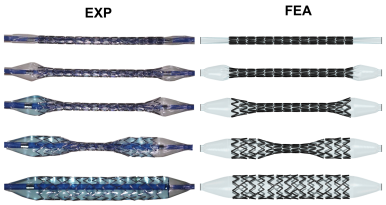

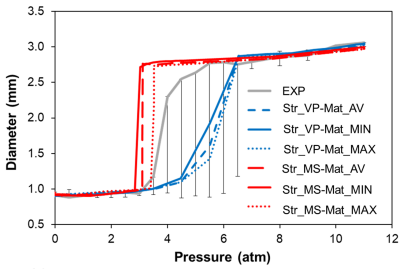

3) Deployment into PVC tubes

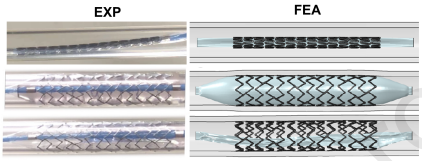

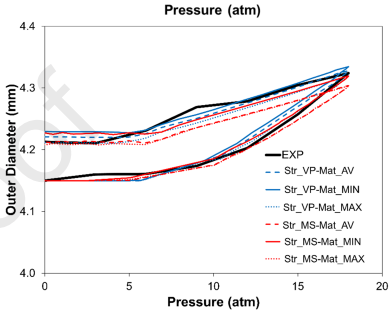

1. Title page: Validation of the computational model of a coronary stent: a fundamental step towards in silico trials

Luca Antonini[1*], Lorenzo Mandelli[1*], Francesca Berti[1], Giancarlo Pennati[1], Lorenza Petrini[2,Δ]

[1] Laboratory of Biological Structure Mechanics, Department of Chemistry, Materials and Chemical Engineering “Giulio Natta”, Politecnico di Milano, Piazza Leonardo da Vinci 32, 20133 Milano (Italy)
[2] Department of Civil and Environmental Engineering, Politecnico di Milano, Piazza Leonardo da Vinci 32, 20133 Milano (Italy)

*Authors contributed equally

Author email address:
Luca Antonini: luca.antonini@polimi.it
Lorenzo Mandelli: lorenzo.mandelli@polimi.it
Francesca Berti: francesca.berti@polimi.it
Giancarlo Pennati: giancarlo.pennati@polimi.it
Lorenza Petrini: lorenza.petrini@polimi.it

Corresponding Author:
[Δ] Lorenza Petrini, Tel.: +39 02 2399 4307; fax: +39 02 2399 4286.

Conflict of interest
None.

2. Abstract and key terms

The proof of the reliability of a numerical model is becoming of paramount importance in the era of in silico clinical trials. When dealing with a coronary stenting procedure, the virtual scenario should be able to replicate the real device, passing through the different stages of the procedure, which has to maintain the atherosclerotic vessel opened.

Nevertheless, most of the published studies adopted commercially resembling geometries and generic material parameters, without a specific validation of the employed numerical models.

In this work, a workflow for the generation and validation of the computational model of a coronary stent was proposed. Possible sources of variability in the results, such as the inter-batches variability in the material properties and the choice of proper simulation strategies, were accounted for and discussed. Then, a group of in vitro tests, representative of the device intended use was used as a comparator to validate the model.

The free expansion simulation, which is the most used simulation in the literature, was shown to be only partially useful for stent model validation purposes. On the other hand, the choice of proper additional experiments, as the suggested uniaxial tensile tests on the stent and deployment tests into a deformable tube, could provide further suitable information to prove the efficacy of the numerical approach.

Balloon-expandable stent; in silico model; finite element model, in vitro tests

3. Introduction

During the conception and development of a medical device, the common practice based on the standard regulations requires defining an experimental study aimed at the evaluation of the overall performances of the device. These tests can range from in vitro investigations (i.e. the mechanical response of the device (BSI, 2012)) to pre-clinical animal studies (i.e. the evaluation of the biological and functional behavior). If the former is controllable but far from the clinical reality, the latter can be extremely expensive and, at the same time, not easily achievable. In the last few years, in silico studies have been coupled with these experimental investigations to account for many factors playing a role in the definition of the device behavior and its interaction with the physiological environment, such as the evaluation of the local stress and strain fields. Hence, nowadays in silico studies are used as a tool to support the design phase of medical devices providing additional/complementary information to in vitro and in vivo investigations. They allow many virtual tests to be performed on the device under specified boundary conditions even before the prototyping phase takes place. Clearly, it is fundamental to guarantee the use of accurate and reliable numerical models in moving towards the substitution of in vitro and in vivo tests with an in silico alternative.

Recent literature (Morrison et al., 2019; Viceconti et al., 2019) and regulatory body publications (ASME, 2006 2018) underline the fundamental role of credibility defined as the trust, obtained through the collection of evidence, in the predictive capability of a computational model for a specified context of use. Indeed, given a question of interest for the specific device, computational models may be used with different roles and scopes to address the question. The process of assessing the credibility of computational models through verification and validation (V&V) recognizes its main aim as the support of programmatic decisions without falling into costly and time-consuming tests. The level of rigor of V&V activities to prove the model's credibility depends on the specific influence that the model itself has on the decisions to be made. In particular, the ASME V&V 40 standard proposes a risk-based framework for establishing the credibility requirements of a computational model for a specific question of interest.

However, before approaching the complex process of assessing the credibility of in silico models it is mandatory to set up a numerical model, able to correctly describe the geometrical and mechanical properties of the device. Validation of the model should be performed using as comparator experimental tests, as much as possible easy to be performed and able to reproduce the device use modalities. Indeed, when setting up an in silico approach, there is an intrinsic dualism that requires, on one hand, a high degree of realism and, on the other hand, its usability. A meticulous description of some features of the real devices can sometimes be considered excessive when the main quantities of interest are not sensitive to these details while the computational time is significantly affected.

This study focuses the attention on metallic balloon-expandable stents used in the Percutaneous Coronary Intervention (PCI) procedure, which is the clinical gold standard for the treatment of occlusive disease due to atherosclerosis (Lee et al., 2008; Vlaar et al., 2007). In the preceding decades, literature about stents has provided a large number of examples of in silico studies investigating different aspects, from the mechanical performances of the device standalone (Lally et al., 2005; Schiavone et al., 2014; Zhao et al., 2012) to the interaction with human arteries (Mortier et al., 2010; Martin and Boyle, 2013, 2011). However, these works were mainly devoted to show the potentialities of numerical models. without any assessment of the model capacity of correctly describing the studied problem.

Only recently, researchers started to approach the theme of balloon-expandable coronary stents numerical models validation. A common choice involves the simulation of a free expansion test, mimicking the experimental procedure of balloon inflation, up to the nominal pressure, and stent opening without any radial constraint (e.g. tube or arterial wall). It is a controllable test, also required by technical standards (e.g. ISO), allowing the user to measure the stent pressure - diameter curve and its behavior when fully expanded by the balloon. In the recent work of Geith et al. (2019), the authors performed an extremely realistic simulation, involving the careful reproduction of the balloon folding procedure prior to the stent crimping phase to account for all the residual stresses arising in the balloon. They compared this new approach with others available in the literature, obtaining different curves sharing the initial and final trends (i.e. the starting and expanded diameter of the stent) but with a different dynamic phase (defined as the balloon opening phase with the typical “dog-boning” effect at its extremities). The validation consisted of the comparison of all the numerical outputs with one experimental curve from a free expansion test, demonstrating an almost perfect match. However, supported by the literature study by Qiu and Zhao (2018), there is a wider dispersion in the diameter measurements taken in the dynamic phase, which could have led to a different conclusion regarding the justification of the use of such a complex model.
Another work exploiting the free expansion tests is by Wiesent et al. (2019), which performed eight experiments on two different stent geometries, focusing on aspects affecting the pressure-diameter curve such as the design and misalignment. As in the previous case, a lot of effort was spent in the preparation and validation of the realistic folded balloon model, which might be not necessary when the interest is in the mechanical performance of the stent. Indeed, it must be considered that usually the purpose of a stent's simulations is to predict its behavior when implanted in an artery. Therefore, an in silico model of a balloon-expandable coronary stent has to be able to take into account those aspects influencing the stent capability of maintaining open a stenotic artery, such as the residual stresses induced during the crimping procedure and the radial stiffness. Once verified those aspects are correctly described, it is possible to move towards more complex simulations, addressing different questions of interest, also considering the stent deployment in a virtual

patient, where an excellent mimicking of the stent-vessel interaction is required.
With few exceptions (Bukala et al., 2017; Debusschere et al., 2015), the majority of free expansions simulations available in the literature (Conway et al., 2017; Gastaldi et al., 2010) were performed exploiting an explicit solver to have reasonable CPU times and acceptable results, as long as proving that the choice of the numerical parameters led to a quasi-static condition. However, the results of the simulations may be affected by the numerical strategies adopted.

With this awareness, the purpose of this work is twofold. First, to define a rigorous and feasible workflow to build a validated computational model of a metallic balloon-expandable stent, ready to be used to address different questions of interest and to be subjected to the credibility assessment. Second, to assess how the uncertainties of the material properties and the selection of numerical parameters may influence the simulation results and validation process. These two aims will be exemplified referring to a specific commercial coronary stent.

4. Materials and methods

The suggested framework for the development and validation of a virtual coronary stent is exemplified considering a specific drug eluting balloon-expandable device: SYNERGY™ BP (Bioabsorbable Polymer) Everolimus-Eluting Platinum Chromium Coronary Stent, by Boston Scientific Limited (BSL). Indeed, this work was developed in the context of the “Insilc” project funded by the European Commission, where the author’s role was the numerical study of coronary stents deployment in virtual patients: thanks to the presence of BSL as a partner, it was possible to have some samples of SYNERGY™ BP stent for validation purposes. In particular, five complete delivery systems, i.e. crimped stents on a balloon and catheter, all belonging to the same batch, were made available for this study, together with data regarding the stent geometry.

The experimental study was defined to maximizes the information obtainable for the validation of the in silico stent model by comparing the numerical outputs with the experimental data. In particular, the literature standard free expansion tests were preferred, allowing to be coupled with uniaxial tensile tests on the stents in the post-expansion configuration: four out of the five available delivery systems were used to better account for the experimental variability. Both these tests are also required by the technical standards for characterizing the mechanical behavior of the device. The last stent was deployed into a deformable PVC tube, for testing the device in conditions resembling the clinical use. Since the stent material is not sensitive to temperature and humidity, all the experimental activities were performed in air and at environmental temperature. Moreover, further tests were necessary for calibrating the mechanical properties of the balloon and the PVC tube required as inputs of the FE model.

The numerical simulations were performed using the commercial code ABAQUS 2018 (Simulia Corp. USA)

4.1 Experimental study

4.1.1 Stent free expansions

Four free expansion tests were performed following an ad-hoc protocol to obtain the diameter-pressure curve. The set-up comprised (Figure 1): a syringe pump (PHD 2000, Harvard Apparatus, maximum pressure 7 atm) equipped with a 1 ml glass syringe (Hamilton–Microliter Series Gastight); an infusion syringe (MEDFLATOR, Inflation Syringe System, MedexTM); a pressure transducer (piezoresistive pressure sensor, Honeywell Sensing and Control) connected to a data acquisition board, two three-way stopcocks and a high-resolution camera (Canon EOS 6D) equipped with a macro-objective (Canon MP-E 65mm f/2.8 1-5x). Since the syringe pump was run in controlled-volume mode, syringe inner diameter, target volume, and infusion/refill rates needed to be set so that the pump automatically calibrated the plunger displacement to provide the desired flow rate. Due to the limit in the pressure of the syringe pump, and to avoid damage to the pressure transducer, during the experiment, once the value of 7 atm was reached, the pump was switched off, closing the connection with the transducer. At this stage, the connection with the inflator (properly pressurized) was opened and the screw of the infusion syringe turned to generate pressure up to the desired value (nominal 11 atm, up to a maximum of 20 atm). The pressure value was acquired directly from the inflator's manometer.

Distilled water was used as an inflation medium and alimentary dye allowed visualization of the presence of liquid inside the catheter and balloon. The tip of the catheter, which accommodated the delivery system, was fixed at its extremities to avoid longitudinal and circumferential displacements thus allowing balloon free expansion in the radial direction.

The air inside the system was carefully removed as a source of possible variability in the results.

For the analysis of the results, the video was first synchronized to the acquired pressure data, then frames in correspondence to specific pressure values are extracted with MATLAB software (MATLAB and Statistic Toolbox Release 2017b, The MathWorks, Inc., Natick, Massachusetts, United States). To perform a detailed analysis of the diameter deformation, each frame was analyzed with ImageJ software (National Institute of Health, USA). Measures of the stent's inner diameter were acquired respectively on the central segment at targeted pressure values. To account for inter-user variability, multiple measurements were taken, and the diameter value

was obtained as an average. Data variability was accounted for as the range between minimum and maximum measurements.

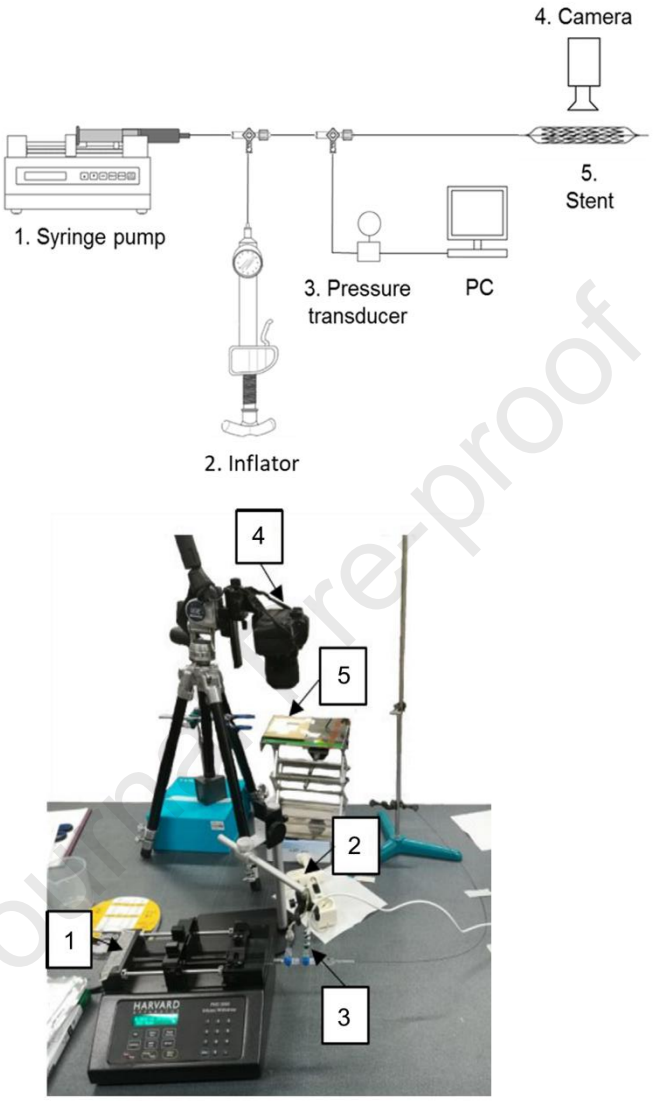

Figure 1 Experimental set-up, composed of (1) a syringe pump, (2) an inflator, (3) a pressure transducer, (4) a high-resolution camera, (5) the device (balloon + stent or balloon only).

4.1.2 Uniaxial tensile tests on post-expanded stents

After the free expansion, the four stents were subjected to uniaxial tensile testing using BOSE Enduratec ElectroForcer® 3200, mounted with a 22 N load cell. Uniaxial tensile tests consisted of a loading phase in displacement control of up to 3 mm. The stents were glued at their extremities onto proper supports (cylindrical rods with a size equal to the internal diameter of the expanded devices) that were directly clamped into the testing machine. Particular care was paid to obtain a repeatable gauge length for testing. This test allowed investigation of the axial stiffness of the

expanded stent, which plays a role when the device is implanted into the vessel, and to investigate the effects of residual stress and strain fields due to crimping and inflation on the device mechanical response (force-displacement curve).

4.1.3 Stent deployment into a PVC tube

Using the last available delivery system, one constrained deployment test of a stent into a PVC tube was performed. The same experimental set-up previously described for the free expansions was used. A commercially available PVC tube (lumen = 3.05 mm, wall thickness = 0.55 mm) was selected to reasonably mimic the coronary artery in terms of lumen dimension. The tube was positioned fixing its extremities inside rigid support. In contrast to what was done for the free expansion, in this case, the stent was expanded by inflating the balloon to a pressure up to 18 atm. Three optical acquisitions of the outer tube diameter were recorded by two different operators to evaluate the inter-operator variability. The quantities of interest were the vessel's outer diameter at maximum balloon inflation and after stent deployment: the former, when dealing with stent deployment in patient-specific arteries, can be considered as an indicator of the wall damage, while the latter refers to the vessel lumen patency post stenting.

4.1.4 Calibration tests

To calibrate the balloon and PVC tube mechanical properties, the following tests were also performed.
Since the available delivery system balloons were mounted on the catheter with the stents, at the end of the stent free expansion tests, the four deflated balloons were tested again, following the same protocol previously described, to obtain their pressure-diameter curves up to 20 atm. The results of the tests are reported in the Appendix.
Three 5 mm long tubular samples were used for the PVC material model calibration through an annular tensile test, in displacement control (0.05 mm/s), up to 4 mm. Force-displacement data were acquired.

4.2 Development of the finite element models

Even if BSL provided the whole delivery system of SYNERGY™, the catheter played a marginal role in the performed tests. Hence, as a first approximation, its presence was neglected in the simulations.

4.2.1 The SYNERGY^{TM} BP stent

The geometrical model of the SYNERGY^{TM} BP stent was provided by BSL in its unstressed configuration (namely, at the end of all the manufacturing processes, pre-crimping). It had a length of 16.4 mm and an external diameter of 1.8 mm, as the tube used for laser-cutting. The strut section was 89 μm in width and 79 μm thick

(**Figure 2a and 2b**). After crimping and expansion, this stent has a nominal inner diameter of 3 mm.

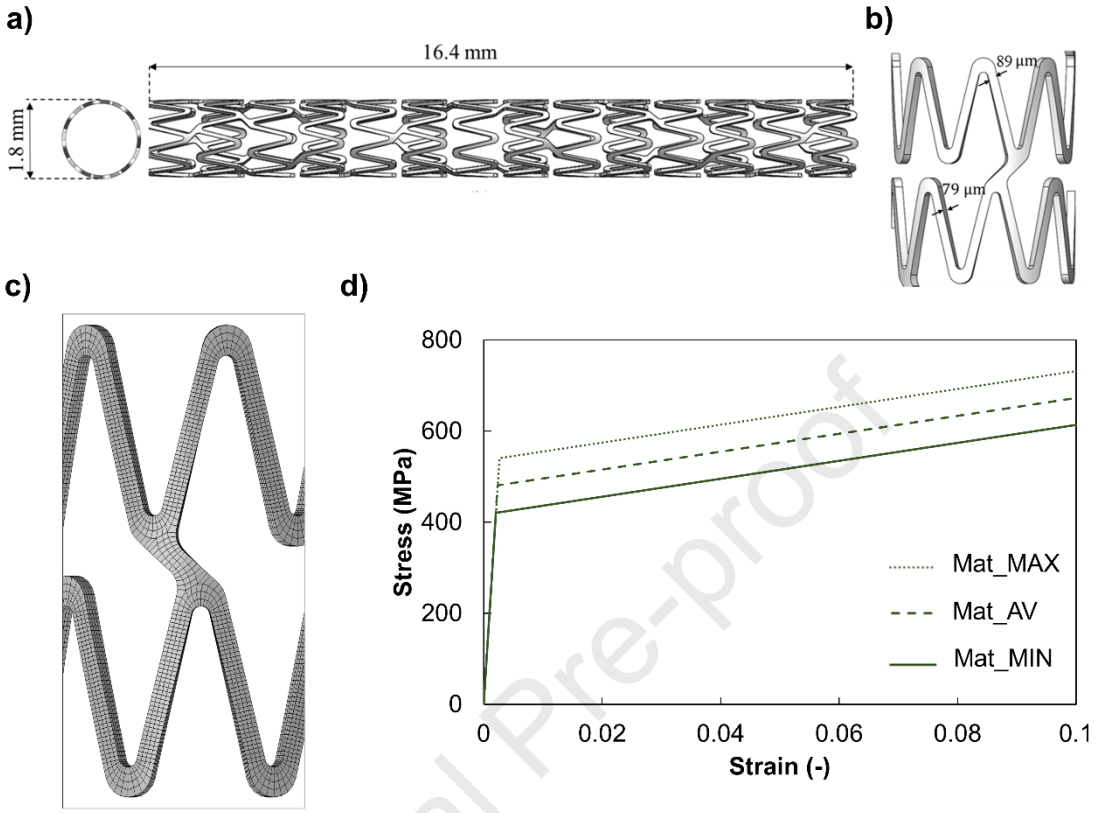

Figure 2 SYNERGY™ BP geometry in the pre-crimping configuration: a) frontal and lateral view; b) detail showing strut width (89 µm) and radial thickness (79 µm); c) detail of the stent meshed according to the chosen refinement; d) different material properties used in the study for accounting inter-batch variability.

In principle, also the polymeric coating should be accounted for in the stent FE model. Nevertheless, its effect on the mechanical response of the stent during crimping or deployment is marginal, since the abluminal coating thickness is very thin (approximately 4 µm for the SYNERGY™ BP stent) compared to the strut radial thickness and the mechanical stiffness of the polymer is considerably lower than that of the metal alloy of which the stent is made. Indeed, stent expansion is mainly driven by the stent radial stiffness which, in turn, depends on the stent backbone material and cell design. This was confirmed in a study (Schiavone et al., 2014), that evidenced how, in metal stents, drug-eluting coatings have a limited effect on stent expansion, recoiling, dog-boning and residual stresses. Therefore, in this study, the drug-eluting coating was not considered. Conversely, since during the in vitro validation phase of this study, the stent was deployed within a PVC tube, in this section also the model of such a tube is presented and discussed.

Due to their specific geometrical pattern, stent meshes might be easily built starting from two basic elements: the V-shape unit and the link. The software used for this

task was HyperMesh (Altair Hyperworks, 2017). The finite element grid was created on the external surface of the V-shape unit and then extruded through the thickness of the strut. The same process was applied to the link: it was partitioned in this manner to support the construction of the mesh without the generation of distorted elements, then the surface mesh was created and extruded.
By replicating the V-shape and the link units, the whole mesh was obtained. The quality of the mesh was checked through the Jacobian index, which quantifies the deviation of an element from an ideally shaped element. Hexahedral elements with reduced integration (C3D8R) were chosen since this element formulation is particularly suitable for all those analyses where bending is the most relevant loading condition. In addition to that, to avoid mesh distortion during the simulation steps, both a distortion control and an hourglass enhanced control were activated. The whole model was discretized with 177312 elements (meaning a 4x4 refinement in the strut cross-sections) after a mesh sensitivity analysis (**Figure 2c**).

The SYNERGY™ BP stent is made of a platinum-chromium alloy (Pt-Cr) which exhibits a bi-linear elastoplastic behavior. For the material parameter values of this device, the manufacturer suggested referring to the data reported in (O'Brien et al., 2010). However, the mechanical properties characterizing the plastic behavior of the Pt-Cr alloy are dependent on the annealing process. This means that the stent obtained from different tube batches may have very slightly different properties. Unfortunately, it is not feasible to associate the exact material properties to each batch and, hence, delivery system. For this reason, in this work other two sets of materials properties were considered, having the same elastic properties and hardening, but different values of yield stress, aiming to explore the variability of the material plastic behavior. Accordingly, in **Table 1** are reported the literature parameters, corresponding to the average material response and hence indicated as "Mat_AV", and the parameters defining the lower and upper limit of the behavior variability range, indicated as "Mat_MIN" and Mat_MAX", respectively. The corresponding stress-strain curves are reported in **Figure 2d.**

Table 1 Material parameters as in (O'Brien et al., 2010) ("Mat_AV"), then extended for considering variability in different Pt-Cr tube batches ("Mat_MIN" and "Mat_MAX")

	Mat_AV	Mat_MIN	Mat_MAX
Elastic Modulus, *E* (GPa)	203	203	203
Yielding Stress, σ_y (MPa)	480	420	540
Ultimate Tensile Strength, *UTS* (MPa)	1208	1148	1268
Ultimate Tensile Deformation, ε_{UTS} (-)	0.37	0.37	0.37
Density, ρ (g/mm^3)	9.9	9.9	9.9

4.2.2 The PEBAX® balloon

The strategy adopted to model the balloon consisted of producing an equivalent component that exhibits the same behavior as the real one: the purpose of the balloon is to allow the stent expansion up to a certain diameter, depending on the inflated pressure. To this purpose, there is no specific interest in the evaluation of local quantities in the balloon, such as stress and strain fields arising from the folding, which seems to affect only the dynamic phase of the stenting procedure with minor influences on the final stent diameter. For this reason, the complexity related to the replication of the real balloon folded structure was not considered. Hence, a multi-wings geometry, slightly tapered at the extremities, with the same length and expanded diameter of the real balloon (**Figure 3**) was adopted following the previous studies (Chiastra et al., 2018; Morris et al., 2018). The geometrical dimensions of the balloon were defined according to the information provided by the manufacturer and to measurements taken on images recorded during the experimental free inflation of the device (see Appendix). The dimension of the folded diameter was defined according to the inner diameter of the crimped stent. The values are summarized in **Table 2**.

Table 2 Balloon dimensions

	Value
Folded Diameter, D_{fold} (mm)	0.9
Unfolded Diameter, D (mm)	2.6
Total Length, *L* (mm)	24.1
Central Length, $L_{central}$ (mm)	16.6

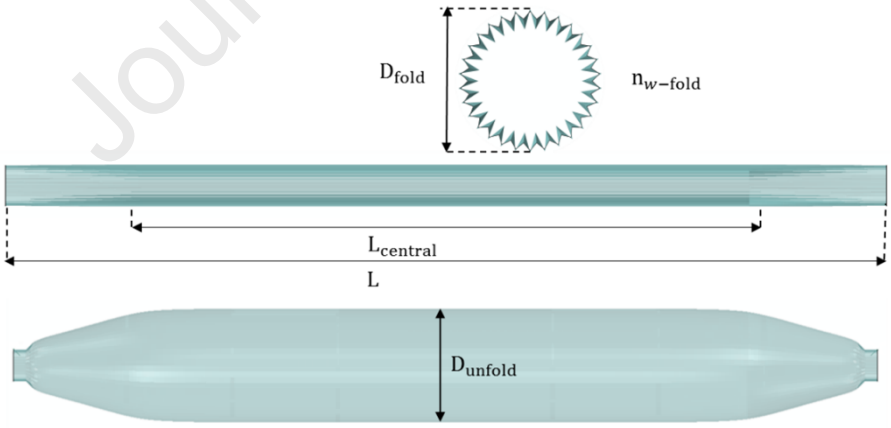

Figure 3 The simplified balloon model.

The discretization of the balloon geometrical model was performed through the HyperMesh software. The final mesh consisted of 14520 membrane elements (M3D4) The full integration formulation was chosen to avoid hourglass effects during the inflation step. The measurement of the thickness of the balloon was taken through a micrometer and was found to be equal to 0.025 mm, a value which was assigned in the model section definition.

The material behavior was described using a hyperelastic Ogden 1st order model for incompressible material, having the following strain energy function:

$$\Psi = \frac{2\mu}{\alpha^2}(\lambda_1^\alpha + \lambda_2^\alpha + \lambda_3^\alpha - 3)$$

where λ_i are the principal stretches, μ and α material parameters. These parameters were calibrated by replicating in silico (using ABAQUS/Explicit) the balloon free expansion tests (Section 4.1.4 Calibration tests) and matching the experimental data with numerical results, as described in the Appendix. The adopted material parameters were μ=80 and α=-15.

4.2.3 The PVC tube

The tube geometry was designed using Solidworks (Dassault Systèmes, France) and discretized in hexahedral elements, reduced integration, through Hypermesh.
It was discretized with 28250 linear hexahedral elements (C3D8), with three elements in the wall thickness.
The simulation of the annular tensile tests of the PVC tube was used to calibrate the material parameters of a linear elastic constitutive model over the force-displacement average experimental curve (see Section 4.1.4 Calibration tests). To replicate the metal rods pulling the annular sample in the experimental test, two rigid cylinders with a diameter equal to 1.4 mm (the same as the supports used for the experimental tests) were created as discrete rigid bodies and meshed with 522 bilinear rigid quadrilateral elements (R3D4). A surface-to-surface contact ruled the interaction between the cylinders and the sample, defined as independent and dependent surface, respectively. The parameters were set as E=13.5 MPa and v=0.47 (**Figure 4**), allowing us to obtain a good match between the experimental and numerical curves: the maximum deviation of the numerical outcome was detected at 3 mm displacement (17.08 N compared to the 16.14 N of the experimental average curve). The percentage error at the end of the loading phase (4 mm displacement) was lower than 1%.

a)

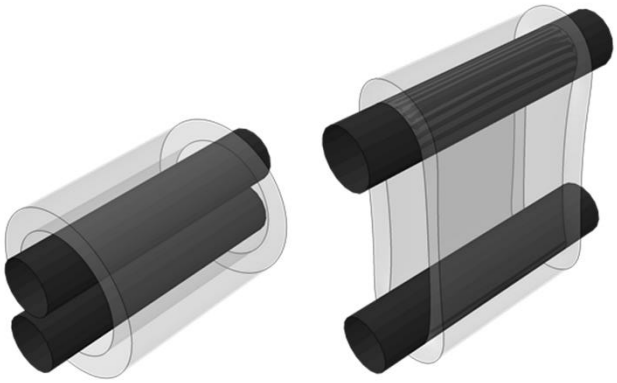

b)

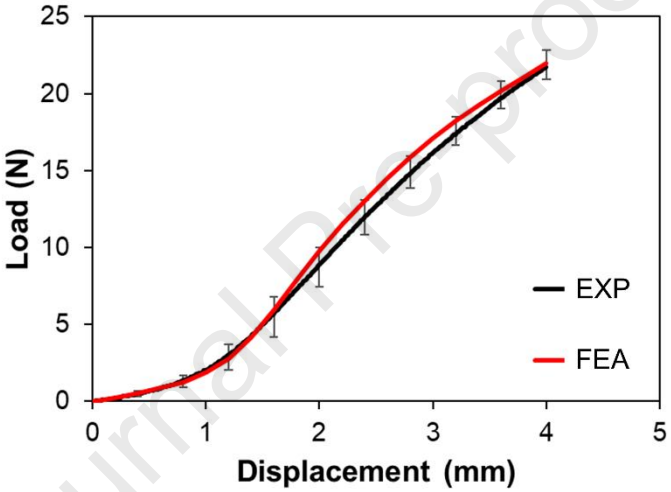

Figure 4 a) Initial and final configuration of the computational annular tensile test of the PVC tube sample and b) the comparison between experimental and numerical results in terms of load-displacement curves. In the experimental curve, the mean value and the maximum and minimum deviation calculated on four tests are shown.

4.3 Numerical simulations for model validation

In clinical practice, it is not possible to distinguish between delivery systems containing stents belonging to different batches. For this reason, all the computational simulations were performed by assigning all three sets of material parameters indicated in **Table 1** to the stent, in order to comment on the potential influence of the material variability due to the annealing process on the test results.

4.3.1 Stent free expansions

The numerical simulation of the system free expansion was performed according to the experimental procedure. Due to the high non-linearities of the simulation, the ABAQUS/Explicit solver was used. However, the crucial aspect of these simulations

is to guarantee a quasi-static condition, through the monitoring of the values of the kinetic energy and internal energy, and, at the same time, to have reasonable CPU times. There are several strategies for achieving this, that could influence the simulation dynamics at some stage, but there is little regarding this in the literature. In this work, two different numerical strategies, aimed at ensuring a quasi-static condition, were investigated: in the first case, the simulation was performed by applying a viscous pressure (3E-5 MPa) on the stent's surface and it is indicated in the following as "Str_VP"; in the second one, the use of a semi-automatic mass scaling (the stable time increment was fixed as 5E-7 s and the density was consequentially scaled) was adopted and is indicated in the following as "Str_MS". Moreover, a step-wise sigmoid amplitude was used for the definition of the loads' boundary conditions. It is worth pointing out that such numerical strategies are allowed in simulations that aim to reproduce phenomena not significantly influenced by viscous effects, as well as simulations involving a stent composed of a metal alloy, such as in the case of this work. On the other hand, dealing with strain rate dependence effects would have necessarily implied a faithful replication of the load rate. Under this consideration, it was also decided to choose a shorter step time with respect to the realistic stent expansion time because, once the quasi-staticity of the simulation is guaranteed, the described physical phenomena are not affected by the duration of the step. Indeed, this led to a considerable reduction in CPU time.

In both cases, a preliminary simulation was performed to crimp the stent model onto the balloon and obtain the delivery system ready for the expansion. The stent crimping was performed by reproducing the effect of a crimping machine through sixteen analytical planes moving radially. The displacement was iteratively changed to reach a stent post-release (after the elastic recoil was allowed by removing the planes) internal diameter equal to the real one (Dcrimp = 0.9 mm).
The stent expansion was performed by applying a progressively increasing uniform pressure up to 11 atm on the internal surface of the balloon, the same pressure applied during the experimental activity. During this phase, the extremities of the balloons were fully constrained to reproduce the balloon fixation on the catheter. To account for the interactions between different parts, balloon-stent, stent-self, and balloon-self contacts were activated. Finally, the pressure was reduced progressively down to a slightly negative value to obtain the balloon deflation and to allow the elastic recoil of the stent. Contact settings were left unchanged with respect to the previous step.
A comparison between the experimental and computational pressure-diameter curves was performed.

4.3.2 Uniaxial tensile tests on expanded stents

For all three stent models and both the numerical strategies "Str_VP" and "Str_MS", the expanded configurations equipped with the residual stress-strain state deriving from the free expansion simulations were imported into ABAQUS/Standard and the

tensile test was performed reproducing in silico the same constraints of the experimental test (namely, the same gauge length was guaranteed by constraining those stent rings that were fixed to the cylindrical supports). Two stent rings both on proximal and distal ends were rigidly bounded to two reference points (RPs) through Multi-Points Constraints (MPCs), to simulate the real constrain. One of the reference points was constrained to avoid all displacements and rotations (encastre) while a linear ramp of 3 mm longitudinal displacement was applied to the other one. Specifically speaking, an MPC is used to constrain the motion of the nodes of a region to the motion of a point. In this simulation, an MPC-type beam was set to constrain the displacement and rotation of the stent terminal rings nodes to the displacement and rotation of the RP through two RPs connected through MPCs to the stent proximal and distal rings. The comparison between the experimental and computational force-displacement curves was performed.

4.3.3 Stent deployment into a PVC tube

The numerical simulation was performed in ABAQUS/Explicit exploiting the results of the crimping procedure performed for the free expansion: the delivery system was positioned inside a 50 mm long PVC tube. Similar to the previous case, using both the numerical strategies “Str_VP” and “Str_MS”, the stent was expanded inflating the balloon applying a progressively increasing internal pressure up to 18 atm; after the balloon deflation, the stent maintained the tube open. A comparison between the experimental and computational pressure-diameter curves was performed.

5. Results

5.1 Stent free expansions

Among all the tests, it was possible to obtain one symmetric expansion, meaning that the dog-boning effect started simultaneously at the extremities (**Figure 5a**). On the other hand, the other three tests showed different degrees of asymmetric expansions, meaning that the stents opened at different values of pressures at their extremities: this could be caused by the presence of residual air in the inflation system. It was chosen to analyze and plot the behavior of the central portion of the stent. In particular, referring to **Figure 5b**, the results of experimental symmetric expansion were represented with the solid line, considered as the reference, while the asymmetric behaviors were detected as a variation from this case. The initial portion of the curve (inflation pressure < 3 atm), can be associated with the pressurization of the system, whose stiffness was dominated by that of the stent. Reduced experimental variability was detected at this stage, where almost no diameter changes were measured. Starting from the value of 3 atm, the central portion of the stent started opening: it was possible to notice a greater variability. The final portion of the curve (inflation pressure $\geq$ 8 atm) represents the stent behavior when fully expanded by the balloon. Also, in this case, limited variability and diameter changes were measured.

The experiments and the simulations showed an agreement on the whole pressure-diameter curve. Both the numerical strategies, regardless of the employed material model, recognized the pressure value at which the central portion of the stent started opening, which can be assessed at 3 atm. For validation purposes, the model should be able to reliably describe the stent behavior once deployed into the target vessel. Given the higher uncertainties related to the comparator during the opening phase, the comparison between the experimental and numerical outcomes was performed on the last portion of the curve. At this stage, its expected behavior is also described by the datasheet of the delivery system.

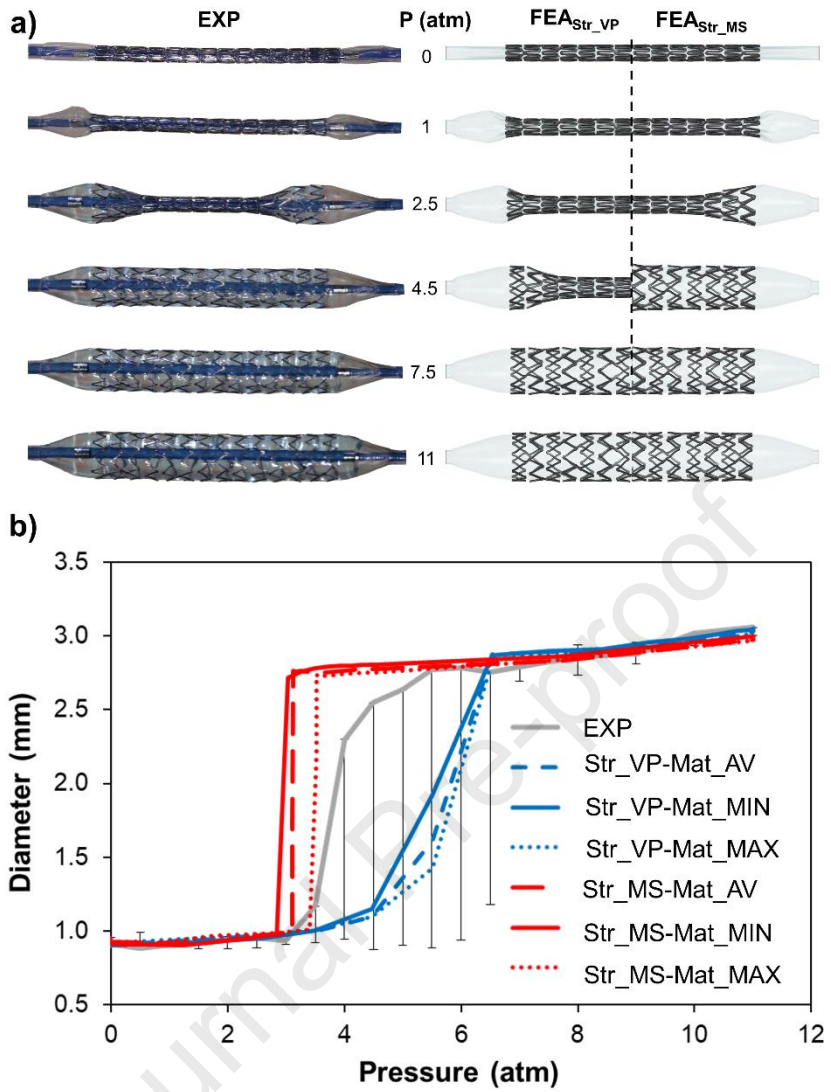

Figure 5 Results of the experimental free expansion tests: a) qualitative comparison of the main phases of the experiment with symmetric expansion and the simulations according to both computational strategies,"Str_VP" and "Str_MS"; b) the pressure-diameter curves according to experiments and different simulations (three material models and two strategies): the experimental solid line represents the case of symmetric expansion with the indication of the maximum and minimum deviation obtained in the other cases

Accordingly, the performance of the model of the delivery system was evaluated based on the comparison between experimental and numerical pressure-stent inner diameter curve at higher pressure, showing an accurate match (**Figure 5b**). In particular, a pressure value of 8 atm represents the first level at which the stent is fully expanded according to both numerical strategies: in both cases, the percentage error with respect to the experimental curve never overcame 2%.

Once the balloon is deflated, a residual state of stress and strain arose in the stent (**Figure 6**). Regardless of the numerical strategy and the material parameters, the most loaded areas belonged to the curvatures of the v-struts. The choice of numerical strategy "Str_MS" led to higher residuals than in the case of "Str_VP",

especially concerning the use of the material “Mat_MIN” (360 MPa compared to 287 MPa, respectively). On the other hand, the increase in yield stress was responsible for higher residuals (e.g. considering the maximum value, from 287 MPa to 339 MPa and 367 MPa in the case of numerical strategy “Str_VP”, and from 360 MPa to 383 MPa and 402 MPa for strategy “Str_MS”).

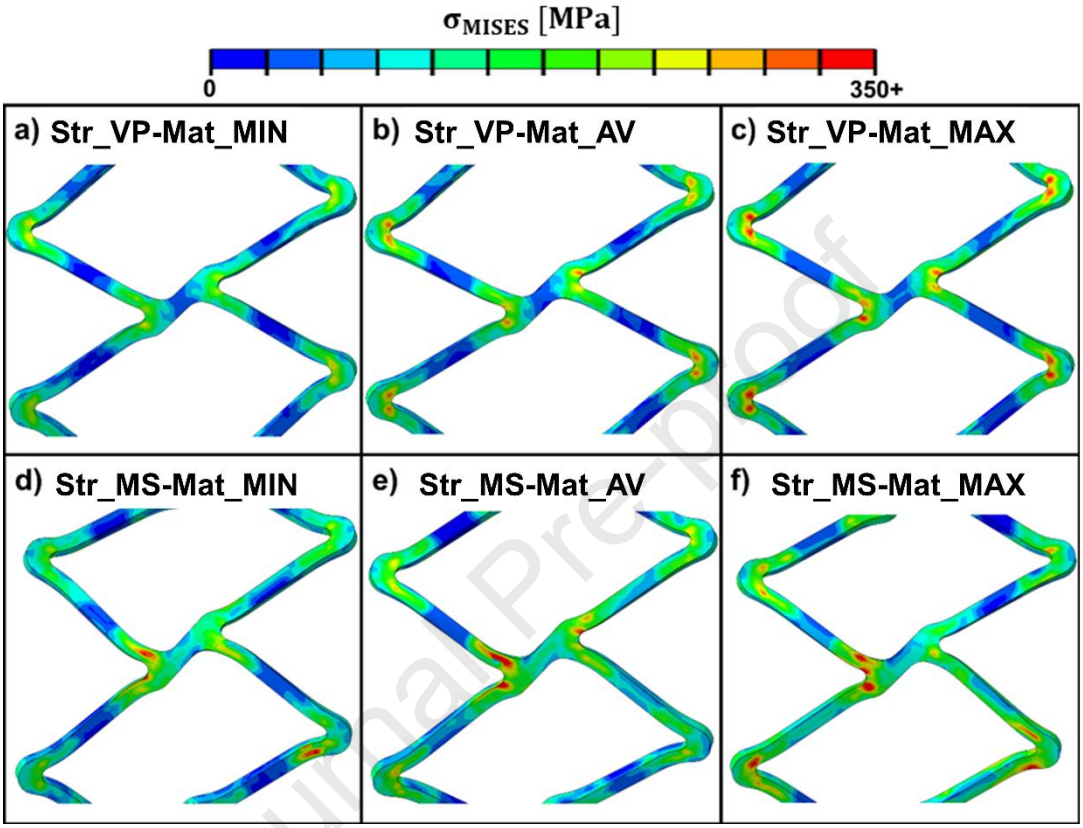

Figure 6 Distribution of residual stresses (σ_{MISES}, in MPa) due to the crimping and free expansion, according to the different numerical strategies and material parameters

5.2 Uniaxial tensile tests on expanded stents

The four stents, tested after free expansion showed an experimental variability especially for the post-yield portion of the curves (**Figure 7**).

The numerical simulations, regardless of the strategy and set of material parameters, matched the initial elastic response, where the main influence on the macroscopic behavior is driven by the geometry, the Elastic Modulus, Poisson’s ratio, and the imposed constraints.

On the other hand, when moving toward higher deformations, the variability increased due to the major influence of the post-yield behavior. The experimental average force measured at 3 mm of displacement was 0.402 N (with minimum and maximum values of 0.356 N and 0.461 N, respectively). The use of the “Mat_AV” and “Mat_MAX” properties led to an under- and overestimation, respectively, of the force

value at 3 mm of 5.5%. A greater variation was found using “Mat_MIN”, with an underestimation of about 16%. The choice of different numerical strategies was responsible for negligible differences, for a maximum percentage difference in the case of the average material properties of 1%.

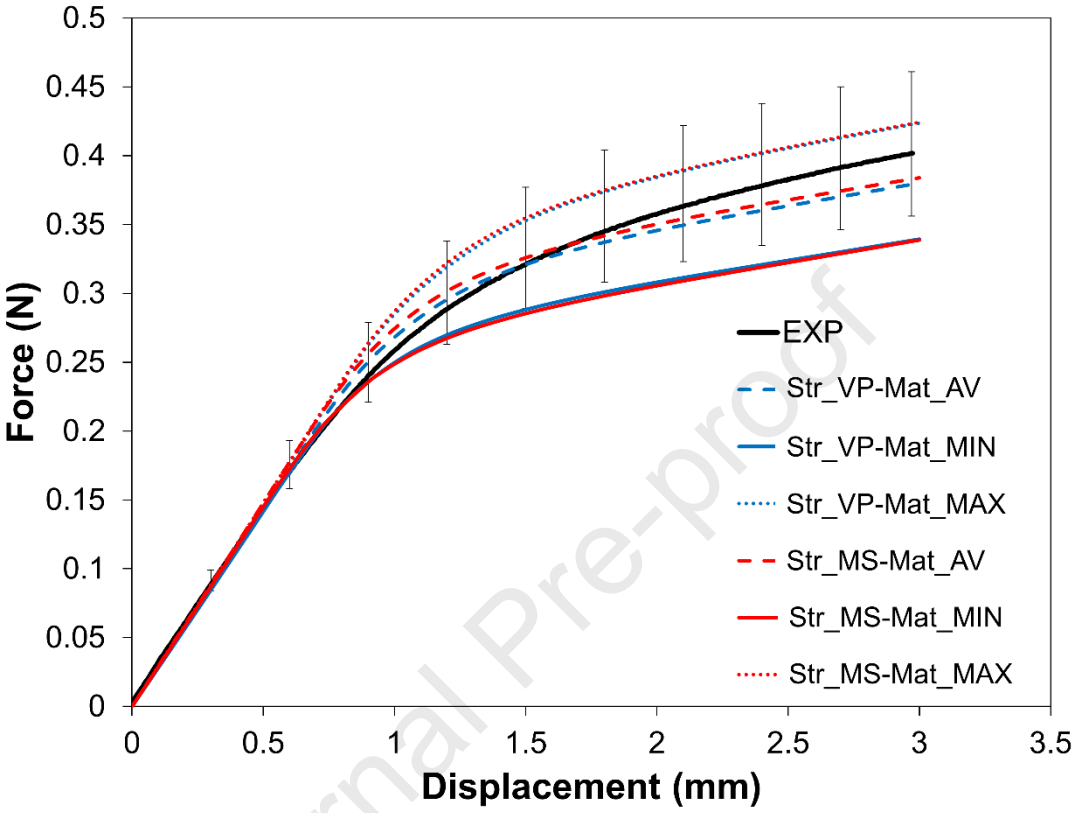

Figure 7 Experimental and numerical results of the uniaxial tensile tests on expanded stents considering two computational strategies and three material models.

5.3 Stent deployment into a PVC tube

The pressure - outer diameter curve detected during the experimental test is plotted in **Figure 8** compared with the results of the simulations. This test represents a more complex scenario compared to the free expansion test, which involves the interaction between many components. The experimental diameter value at maximum inflation was measured as 4.324 mm; at the end of the deployment, it went back to 4.212 mm. The numerical results confirmed a good match, regardless of the choice of different numerical strategies or material parameters. “Str_VP” found slightly higher values than “Str_MS”; both at the maximum inflation and the end of the deflation the percentage error on the predicted diameter never overcame 1%.

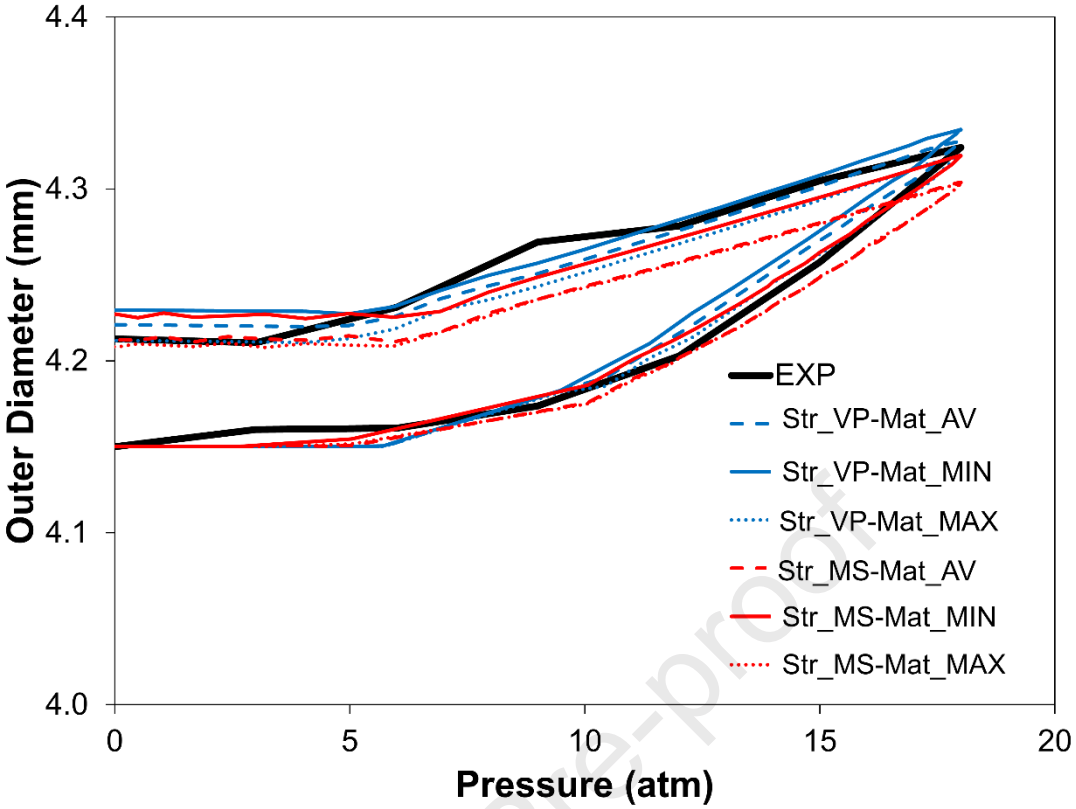

Figure 8 Experimental and numerical results of the deployment into PVC tubes considering two computational strategies and three material models.

6. Discussion

To demonstrate that a computational model accurately represents the behavior of a device, it is necessary to compare the simulated results with well-controlled experiments, able to activate the investigated properties. In this paper, a workflow is proposed to evaluate the ability of a numerical stent model to correctly describe its mechanical behavior with reference to the SYNERGY^{TM} BP stent.

A group of ad-hoc tests allowed the reliability of the model to be proven through the investigation of different aspects, but at the same time having a limited number of specimens. The free expansion test represents the literature gold standard for validation, involving the radial equilibrium between the balloon and the stent; the uniaxial tensile test is an easy experimental procedure, which does not involve contacts between parts except for the machine clamps, and it belongs to those tests used for the verification of the integrity of vascular stents according to ISO 25539-2 (BSI, 2012); last, the deployment in the PVC tube mimics a more realistic scenario, closer to the stent clinical use, which accounts for the interaction with an external constraint, namely the tube wall.

In this work, since the CAD model of the undeformed stent was provided directly by BSL, which is an unusual case for the literature of stents, no uncertainty was present

on the geometry. On the other hand, an intrinsic variability on the plastic properties due to the annealing process of the source tubes was considered.

In agreement with the literature (Qiu and Zhao, 2018), the pressure-diameter curves of the experimental free expansions showed high repeatability in the initial ($p < 3$ atm) and final ($p \geq 8$ atm) portions of the diagram. A greater variability between results was found in the dynamic phase of deployment, which was attributed to factors such as the presence of residual air in the inflation system. The comparison between the numerical and experimental data of the free expansions showed a good match, regardless of the numerical strategy or material parameters employed. The results in the final portion of the plot ($p \geq 8$ atm) are physically related to the interaction between the balloon and the stent, with a major contribution to the result associated with the balloon pressure-diameter characteristics. Since in this work the simulated balloon's behavior was carefully calibrated on multiple experiments, it was expected to find a good match. Moreover, this proved that a simplified balloon model might be effective for these purposes, even if not useful for accurately describing the realistic folding and unfolding phases. On the other hand, the current literature proves the great influence in the experimental dynamic phase of the folding and unfolding, which, however, are intrinsically variable and difficult to predict numerically.

The choice of different numerical strategies, both proven quasi-static, affected the outputs of the simulations in the dynamic phase. For these reasons, validation should be conducted considering those portions of the curves where both the experiments and simulations agreed in less dispersed results. The initial portion of the curve ($p < 3$ atm) depends on the stent behavior only, but the changes in the diameter are barely appreciable and difficult to use. Moving to high pressures, the stent diameter is affected by the deformed configuration of the inflated balloon: the stent diameter values are close to those of the balloon during the free expansions used for calibration, meaning that this phase is mainly controlled by the balloon. The measured stent diameter value differed from the average experimental balloon one for less than 10% for $p \geq 8$ atm. Hence, for the assessment of the device mechanical performance it is necessary to include also tests providing results affected both by macroscopic (diameter) and local (stress and strain fields) variables, and not only by tests dominated by external factors (e.g. the balloon). This was obtained performing uniaxial tensile tests on the expanded stents. However, it is interesting to notice that at the end of the free-expansion, different residual stresses were detected considering different material properties and numerical strategies (Figure 7). In particular, when viscous pressure (Str_VP) is applied, passing from "Mat_MIN" to "Mat_Max" the Von Misies stresses increase coherently, reaching values around 350 MPa in the apex of V-struts. Less predictable is the stress distribution in the case of "Str_MS", with a not clear trend in the stress values varying material properties and larger zones overcoming 350 MPa. It suggests that mass scaling strategy affects the numerical results.

The experimental tensile test results showed a good correlation in the linear portion of the curve, with a higher dispersion for increasing displacement values. Since the stents belong to the same batch, these behaviors are ascribed to small differences in the sample preparation (e.g. micrometric variation in the clamping distance during the preparation, even performed carefully), and to residual stress and strain fields arising during the crimping and free expansion, which are mainly influenced by the choice of the material parameters. The use of different numerical strategies, “Str_VP” and “Str_MS”, did not affect significantly the residual stress and strain fields. The results associated with the “Mat_AV” and “Mat_Max” material properties showed the best results, considering the above mentioned variability. Since the material properties of a specific batch cannot be known before testing, it is reasonable to employ the average set of material parameters specified for these stents in the numerical simulations.

The deployment in the PVC tube allowed a controllable test to be performed that could mimic the clinical use of the delivery system. A limitation of this study is represented by the absence of repetitions of this test, which could have provided details on the experimental variability. However, it was decided to save the majority of the delivery systems for the other experiments. The numerical simulations confirmed the reliability of the model to match the experimental behavior; no significant differences were noticed using the two numerical strategies and the three materials. Even in this case, the use of the average properties led to satisfactory results, especially for the predicted value of the stent diameter at the maximum inflation and at the end of the deployment. Similarly to the uniaxial tensile tests, this test could be effectively exploited for stent validation purposes since the final configuration is strictly dependent on the radial stiffness of the numerical model of the stent itself.

Future efforts will require the extension of the validation process over a wider set of deployment conditions, namely using different deployment tubes (e.g. made of different materials and with different and physiologically inspired geometries), moving toward the evaluation of clinical implantations in human arteries.

7. Acknowledgments

The authors acknowledge Martina Bernini, Alessandra Faicchio, Francesca Gallo, and Agnese Lucchetti for their technical support in the preliminary phase of the work.
The authors would like to thank Boston Scientific Ltd., Co. Galway, Ireland for their collaboration on this work, providing samples and data of the device.
This project has received funding from the European Union’s Horizon 2020 research and innovation program under grant agreement n° 777119. This article reflects only the authors’ view and the Commission is not responsible for any use that may be made of the information it contains.

8. References

ASME, 2018. V&V 40: Assessing Credibility of Computational Modeling Through Verification and Validation: Application to Medical Devices.

ASME, 2006. V&V 10: Guide for Verification and Validation in Computational Solid Mechanics.

BSI, 2012. EN ISO 25539-2 Standards Publication Cardiovascular implants — Endovascular devices Part 2: Vascular stents.

Bukala, J., Kwiatkowski, P., Malachowski, J., 2017. Numerical analysis of crimping and inflation process of balloon-expandable coronary stent using implicit solution. Int. j. numer. method. biomed. eng. 33, 1–11. https://doi.org/10.1002/cnm.2890

Chiastra, C., Grundeken, M.J., Collet, C., Wu, W., Wykrzykowska, J.J., Pennati, G., Dubini, G., Migliavacca, F., 2018. Biomechanical Impact of Wrong Positioning of a Dedicated Stent for Coronary Bifurcations: A Virtual Bench Testing Study. Cardiovasc. Eng. Technol. 415–426. https://doi.org/https://doi.org/10.1007/s13239-018-0359-9

Conway, C., McGarry, J.P., Edelman, E.R., McHugh, P.E., 2017. Numerical Simulation of Stent Angioplasty with Predilation: an Investigation into Lesion Constitutive Representation and Calcification Influence. Ann. Biomed. Eng. 45, 2244–2252. https://doi.org/10.1007/s10439-017-1851-3

Debusschere, N., Segers, P., Dubruel, P., Verhegghe, B., De Beule, M., 2015. A finite element strategy to investigate the free expansion behaviour of a biodegradable polymeric stent. J. Biomech. 48, 2012–2018. https://doi.org/10.1016/j.jbiomech.2015.03.024

Gastaldi, D., Morlacchi, S., Nichetti, R., Capelli, C., Dubini, G., Petrini, L., Migliavacca, F., 2010. Modelling of the provisional side-branch stenting approach for the treatment of atherosclerotic coronary bifurcations: Effects of stent positioning. Biomech. Model. Mechanobiol. 9, 551–561. https://doi.org/10.1007/s10237-010-0196-8

Geith, M.A., Swidergal, K., Hochholdinger, B., Schratzenstaller, T.G., Wagner, M., Holzapfel, G.A., 2019. On the importance of modeling balloon folding, pleating, and stent crimping: An FE study comparing experimental inflation tests. Int. j. numer. method. biomed. eng. 35, 1–19. https://doi.org/10.1002/cnm.3249

Lally, C., Dolan, F., Prendergast, P.J., 2005. Cardiovascular stent design and vessel stresses: A finite element analysis. J. Biomech. 38, 1574–1581. https://doi.org/10.1016/j.jbiomech.2004.07.022

Lee, M.S., Kobashigawa, J., Tobis, J., 2008. Comparison of Percutaneous Coronary Intervention With Bare-Metal and Drug-Eluting Stents for Cardiac Allograft Vasculopathy. JACC Cardiovasc. Interv. 1, 710–715. https://doi.org/10.1016/j.jcin.2008.10.001

Martin, D., Boyle, F., 2013. Finite element analysis of balloon-expandable coronary stent deployment: Influence of angioplasty balloon configuratio. Int. j. numer. Morris method. biomed. eng. 29, 1161–1175. https://doi.org/10.1002/cnm.2557

Martin, D., Boyle, F.J., 2011. Computational structural modelling of coronary stent deployment: A review. Comput. Methods Biomech. Biomed. Engin. 14, 331–348. https://doi.org/10.1080/10255841003766845

Morris, P.D., Iqbal, J., Chiastra, C., Wu, W., Migliavacca, F., Gunn, J.P., 2018. Simultaneous kissing stents to treat unprotected left main stem coronary artery bifurcation disease; stent expansion, vessel injury, hemodynamics, tissue

healing, restenosis, and repeat revascularization. Catheter. Cardiovasc. Interv. 92, E381–E392. https://doi.org/10.1002/ccd.27640
Morrison, T.M., Hariharan, P., Funkhouser, C.M., Afshari, P., Goodin, M., Horner, M., 2019. Assessing Computational Model Credibility Using a Risk-Based Framework: Application to Hemolysis in Centrifugal Blood Pumps. ASAIO J. 65, 349–360. https://doi.org/10.1097/MAT.0000000000000996
Mortier, P., Holzapfel, G.A., De Beule, M., Van Loo, D., Taeymans, Y., Segers, P., Verdonck, P., Verhegghe, B., 2010. A novel simulation strategy for stent insertion and deployment in curved coronary bifurcations: Comparison of three drug-eluting stents. Ann. Biomed. Eng. 38, 88–99. https://doi.org/10.1007/s10439-009-9836-5
O'Brien, B.J., Stinson, J.S., Larsen, S.R., Eppihimer, M.J., Carroll, W.M., 2010. A platinum-chromium steel for cardiovascular stents. Biomaterials 31, 3755–3761. https://doi.org/10.1016/j.biomaterials.2010.01.146
Qiu, T., Zhao, L., 2018. Research into biodegradable polymeric stents: a review of experimental and modelling work. Vessel Plus 2, 12. https://doi.org/10.20517/2574-1209.2018.13
Schiavone, A., Zhao, L.G., Abdel-Wahab, A.A., 2014. Effects of material, coating, design and plaque composition on stent deployment inside a stenotic artery - Finite element simulation. Mater. Sci. Eng. C 42, 479–488. https://doi.org/10.1016/j.msec.2014.05.057
Viceconti, M., Juarez, M., Curreli, C., Pennisi, M., Russo, G., Pappalardo, F., 2019. POSITION PAPER: Credibility of In Silico Trial Technologies - A Theoretical Framing. IEEE J. Biomed. Heal. informatics XX, 1–11. https://doi.org/10.1109/JBHI.2019.2949888
Vlaar, P.J., De Smet, B.J.G.L., Zijlstra, F., 2007. DES or BMS in acute myocardial infarction? Eur. Heart J. 28, 2693–2694. https://doi.org/10.1093/eurheartj/ehm474
Wiesent, L., Schultheiß, U., Schmid, C., Schratzenstaller, T., Nonn, A., 2019. Experimentally validated simulation of coronary stents considering different dogboning ratios and asymmetric stent positioning. PLoS ONE 14, 1–25. https://doi.org/10.1371/journal.pone.0224026
Zhao, S., Gu, L., Froemming, S.R., 2012. On the importance of modeling stent procedure for predicting arterial mechanics. J. Biomech. Eng. 134. https://doi.org/10.1115/1.4023094

9. Appendix: numerical vs experimental free expansion tests of the sole balloon

The balloon free expansion experimental tests (**Figure 1A)**, performed as described in Section 4.1.4, was replicate in silico. In the simulation, the balloon extremities were constrained to avoid any displacement or rotation; the pressure was applied through a smooth step amplitude from 0 up to 20 atm, consistent with the experiments, to the internal surface of the balloon and associated with the corresponding diameter; the values of the kinetic energy and internal energy were monitored to guarantee a quasi-static condition.

Comparing the experimental and numerical pressure-diameter curves (**Figure 2A**) , it is possible to recognize an initial portion of the curve ($p < 1$ atm) which is

representative of the balloon opening phase, with a sudden increase in the diameter value. However, since the balloons were tested after the stent free expansion tests, they did not start from a folded configuration and their initial behavior was affected by great variability due to the unverifiable initial condition (namely, the balloon was deflated and assumed a randomly collapsed configuration as in **Figure 1A**). Due to the simplified geometry, the numerical model was not able to match this very initial condition. Then, an almost linear trend for p ≥ 1 atm referred to effective inflation, where the percentage error of the computational simulation predicted diameter with respect to the experimental value was always lower than 1.5%.

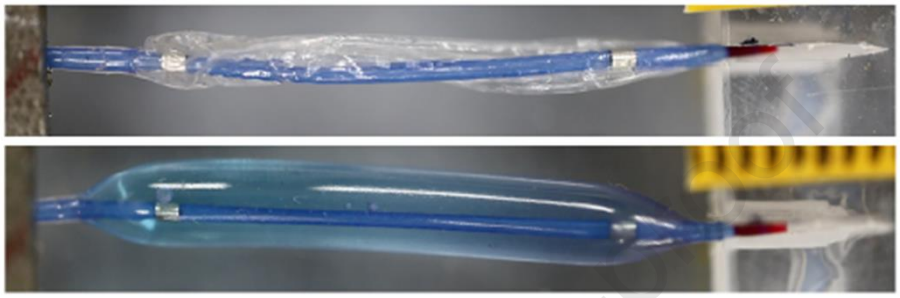

Figure 1A Two pictures of the balloon free expansion test.

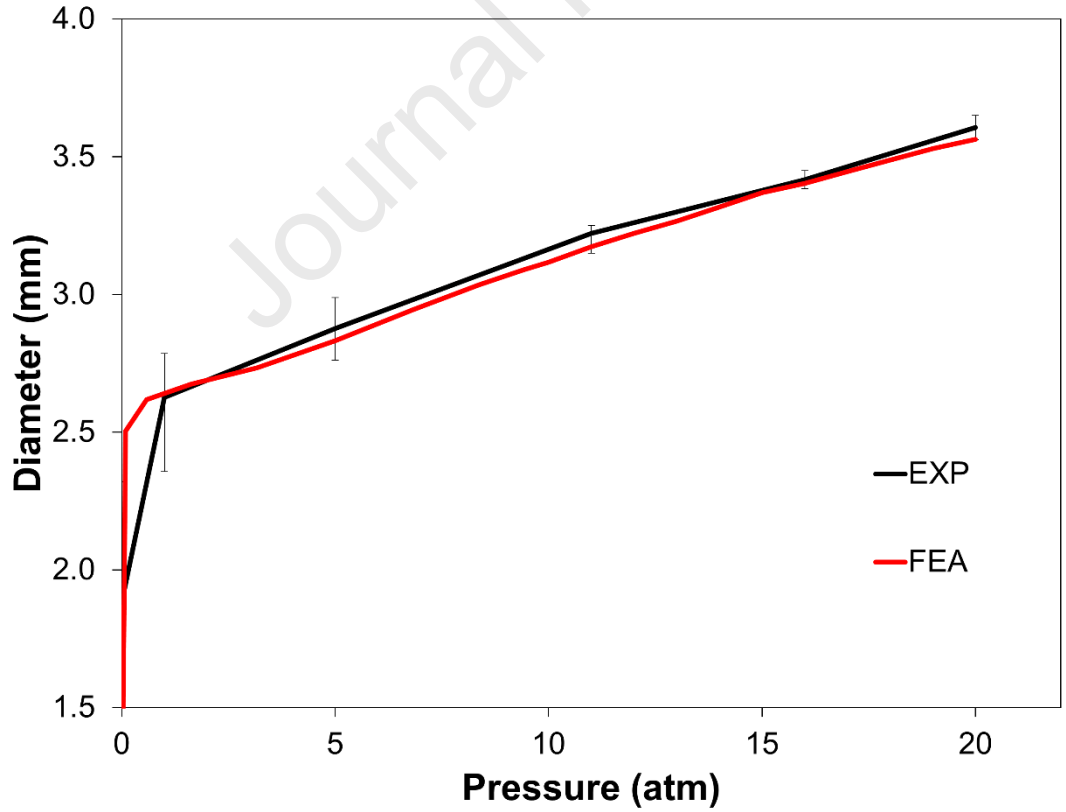

Figure 2A Comparison between the experimental and numerical results of the balloon inflation in terms of pressure-diameter curves. In the experimental curve, the mean value and the maximum and minimum deviation calculated on four tests are shown.

Highlights

1. In the era of in-silico trials the reliability of a numerical model must be proven through the comparison with well-controlled experiments
2. The intrinsic variability of each test has to be critically evaluated when choosing the proper experimental campaign
3. The computational model of a coronary stent delivery system must be able to predict the device capacity of sustaining an injured vessel
4. Modeling simplifications allow to reach good results with a reduction in the computational cost
5. Both macroscopic (e.g. diameter) and local quantities (e.g. stress and strain fields) should be evaluated to prove the numerical accuracy

Declaration of interests

☒ The authors declare that they have no known competing financial interests or personal relationships that could have appeared to influence the work reported in this paper.

☐The authors declare the following financial interests/personal relationships which may be considered as potential competing interests: